Solution of Coupled Electromagnetic and Thermal Problems in Gas Insulated Bus Bar

Suad Ibrahim Shahl [1], Anwer Fouad mohammed Ali[2]

[1] University of Technology, Department of Electrical Engineering,
Baghdad 10066, Iraq
30053@uotechnology.edu.iq

[2]University of Technology, Department of Electrical Engineering,
Baghdad 10066, Iraq

Abstract: ***The magnetic field produced by an alternating current flowing in the conductor of the gas insulated bus bars in gas insulated substations induces eddy currents in the metal parts nearby. The eddy current losses and the outer field can be reduced by optimizing the gas insulated bus bars geometry. This work deals with the influence of gas insulated bus bar enclosure geometry on the power losses and temperature distribution of gas insulated bus bars of substations having separately enclosed bus bars, and since the current carrying capacity of the gas insulated bus bar is limited by maximum operating temperature, it is very important to apply the heat transfer coefficient on the boundary surfaces to predict the temperature distribution in the gas insulated bus bars. The temperature distribution is predicted by coupled magneto-thermal finite element analysis. A harmonic electromagnetic analysis is performed to determine the current losses in the gas insulated bus bar. The electromagnetic analysis is followed by a steady-state thermal analysis to determine the temperature distribution in the gas insulated bus bar; also a fluid analysis has been used to get the temperature distribution of SF_6 gas.***

Keywords: Eddy currents, Finite element method (FEM), Gas Insulated Switchgear (GIS), Gas insulated bus bar (GIB), Electromagnetic -Thermal coupling.

1. Introduction

The basis of Gas Insulated Switchgear (GIS) to supply power to the GIS bus bar is the insulation design and power design. Power design is a technology that enables them to work safely withstanding the thermal stress exerted on the GIS bus bar design. For the power design, conductor and bus bar diameter, tank diameter, tank thickness and shape variables such as the material of the tank, such as the design variables must be determined.

Dielectric limiting factor than the design variables is an even greater impact on the thermal limiting factor. Therefore, it is very important to accurately predict the temperature rise inside and outside rated current GIS bus bar [1].

The advances in insulation technology in the last few decades made it possible to reduce switchgear size to a level that no one could imagine 40 years ago. Moreover, there is a tendency towards using higher rated power units, which require larger conductor sizes. However, the decreasing distance between the active conductors and the enclosures, and the increasing cross sections lead to a more pronounced electromagnetic proximity effect. This can cause higher losses by distorting the current distribution in the live conductors and by inducing eddy currents in the metal enclosures. Moreover, eddy current losses are of the same order of magnitude as the losses in the live conductors [2], therefore, it is very important to reduce them as much as possible. Despite the losses, eddy currents play a major role in mitigating the magnetic field outside the equipment.

The distribution of eddy currents, and consequently the magnitude of both the losses and the outer field, is highly influenced by the equipment's configuration. For specific configurations of gas insulated busbars, the finite element method (FEM) or other sophisticated numerical techniques provide accurate and reliable methods for calculating the electromagnetic field.

Magneto-thermal field analysis is required in many applications such as reactors, induction furnaces, electrical machines and power cables. Knowledge of the temperature profile is important to understanding of the performance and to the improvement of the design of these systems. Different methods have been used for magneto-thermal field analysis. Separate lumped, resistive models used for calculation of magnetic and thermal fields yields approximate results and provide no information about the field distribution. Uncoupled finite element models provide more accurate results and useful information about the flux distribution, especially the temperature profile in the cross section of the system. However, the method does not take into account the interdependence of one field parameters to the second field variation such as electrical conductivity variation due to temperature change. Coupled finite element field analysis, which has been used for thermal analysis of electromagnetic devices [3,4], provides more accurate results than uncoupled methods.

In this work GIS bus bar numerical model based on parameters of 400kV GIS by using three-dimensional FEM is established. Calibration of the numerical model is based on the proposal different structures GIS bus-bar in different operating conditions to mitigate the effect of electromagnetic –thermal coupling. A solution of coupled electromagnetic and thermal problems has been proposed by using load transfer method.

2. **Governing Equations**

For the magneto-thermal field analysis by finite element method, the electromagnetic field will be handled by magnetic time harmonic equations and the thermal field by thermal diffusion equation. The equations relating the various field quantities are constituted by the following subset of Maxwell's equations with displacement currents neglected (quasi-stationary limit):

$$\nabla \times H = J \tag{1}$$

$$\nabla \times \boldsymbol{E} = -\frac{\partial \boldsymbol{B}}{\partial t} \tag{2}$$

$$\nabla \cdot \boldsymbol{B} = 0 \tag{3}$$

where the usual notations have been used for the field vectors. The constitutive relationships

$$\mathrm{H} = \nu \mathrm{B} \tag{4}$$

$$\mathrm{J} = \sigma \mathrm{E} \tag{5}$$

define the material properties where both the reluctivity ν and the conductivity σ may be field-dependent and/or vary in space unless otherwise stated. Hysteresis and anisotropy are neglected [5].

Introducing the magnetic vector potential $\dot{A}$ and the electric scalar potential $\dot{\phi}$ into Maxwell's equation, the 3-D eddy current field equations can be written as [6-7].

$$\left.\begin{array}{ll} \nabla\times(\nu\nabla\times\dot{A})-\nabla(\nu\nabla.\dot{A})+j\omega\sigma_e\dot{A}+\sigma_e\nabla\dot{\phi}=\dot{J}_s & \text{in V} \\ \nabla\cdot\left(-j\omega\sigma_e\dot{A}-\sigma_e\nabla\dot{\phi}\right)=0 & \text{in } \mathrm{V}_1 \end{array}\right\} \tag{6}$$

where V is the whole solution region, V_1 is the region without source current, ν is reluctivity, σ_e is electrical conductivity, and $\dot{J}_s$ is the source current density.

Power-loss is generated at the conductor regions due to the source current and the induced eddy current. Heating-loss should be exactly calculated because power-loss of conductor regions, calculated by the magnetic field analysis, is used as the input data to predict the temperature rise for the thermal analysis [8].

3. Simulation Model

In this work the coupling between the fields can be accomplished by load transfer coupling. A harmonic electromagnetic analysis calculates Joule heating, which is used in a thermal analysis to predict temperature solution. Load transfer ANSYS Multi-field solver algorithm topic is available in the ANSYS Multiphysics product. The schematic flow chart of the implemented algorithm is illustrated in Figure (1) an electromagnetic model and a fluid model are established respectively.

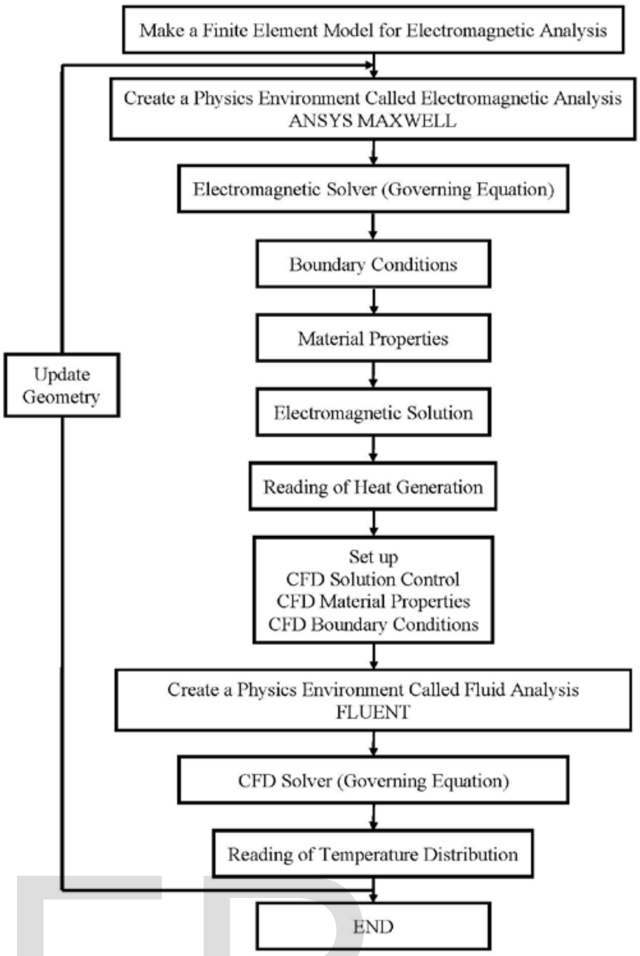

Figure 1: Data flow for a load transfer coupled physics analysis using multiple physics environments

Gas insulated busbar (GIB) consists of main conductor and metallic tank, and SF6 gas fills in between them. In this work all these three main items (Conductor, Tank and SF6 gas) are contribute in both electromagnetic and thermal analysis. Figure (2) shows the cross-sectional view of a single-phase GIB model.

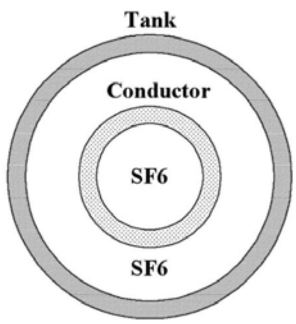

Figure 2: Cross section of a single-phase bus bar model

Tables (1 - 2) show the parameters used in the simulation.

Table1: Parameters of conductor and tank

Model Parameters		*Diameter*	*Value [mm]*
Dimension	conductor	Inner Diameter [mm]	70
		Outer Diameter [mm]	110
	Tank	Inner Diameter [mm]	454
		Outer Diameter [mm]	466
Material Properties		Type	Value
Relative permeability μ_r	conductor	Aluminum	1
	Tank	Stainless Steel	1
Resistivity ρ	conductor	Aluminum	$3.36\times10^{-8}\Omega$ m
	Tank	Stainless Steel	$7.50\times10^{-7}\Omega$ m
Thermal Conductivity [W/m°C]	conductor		148.62
	Tank		43.2
Heat-Transfer Coefficient [W/m^2°C]	conductor		7.5383
	Tank		3.1708
Ambient temperature (^{0}C)	conductor	22	
	Tank	22	
Max operating temperature (^{0}C)	conductor	105	
	Tank	70	

Table 2: Parameters of air and SF6

Parameter	*SF_6 Gas*	*Ambient Air*
Density [kg/m^3]	13.5	1.026
Dynamic Viscosity [m^2/s]	1.31E-6	19.6E-6
Thermal Conductivity [W/m°C]	0.0153	0.0287
Specific Heat [J/(kg.k)]	665.18	1005
Relative permeability μ_r	1	1

Two elements are chosen in this work, 3-D magnetic solid element SOLID97 and 3-D fluid-thermal element FLUID142. SOLID97 is based on the magnetic vector potential formulation with the Coulomb gauge, and has nonlinear magnetic capability for modeling B-H curves or permanent magnet demagnetization curves. FLUID142 is FLOTRAN CFD element use to solve for flow and temperature distributions within a region.

This work presents two models for a single-phase bus bar models depending on geometry parameters of (400kV, 4000Amp, 50 Hz) isolated phase GIB in 400kV gas insulated substation (GIS), as follows:

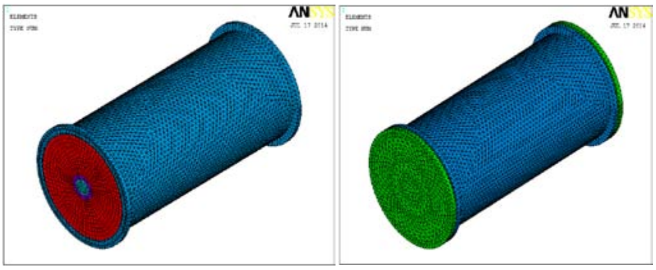

(a) **(b)**

Figure 3: Straight Tube-Shaped GIB Isometric view, (a) GIB's tank with flanges, (b) GIB's tank with flange and cover

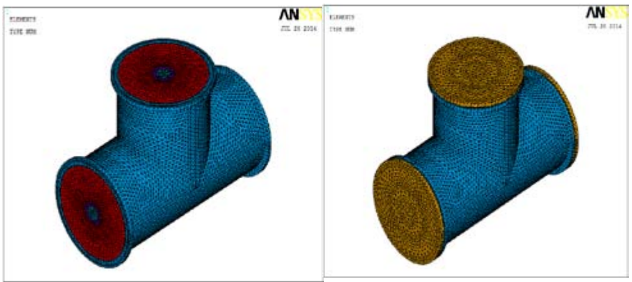

(a) **(b)**

Figure 4: Single Phase T-Shaped GIB, (a) SF6 gas, conductor and tank enclosure, (b) SF6 gas, conductor, SF6 gas, tank (enclosure) and covers

1. Straight Tube-Shaped GIB, Figure (3).
2. T-Shaped GIB, Figure (4).

4. Results and Discussion

In this work, the ANSYS software package version 12.1 is used as the programming environment for gas insulated busbar modeling and analysis. This work deals with the influence of different shape (model) of isolated phase GIB on the power losses and temperature distribution.

4.1. Case Study One: Isolated Phase GIB, Straight Tube-Shaped GIB Model

Figure (5) illustrates the eddy currents density (A/m^2) distribution in the GIB tank (enclosure) with cover get it from the harmonic analysis in vector for real and imaginary solution, it is clear that the major value of GIB tank's eddy currents are concentrating in the longitude axial of the GIB tank body and the minor value are in the Tank's cover.

Tank's power losses (Watt) in contour plot get it from the harmonic analysis which is transferred as heat generation for the thermal analysis as shown in Figure (6). Figure (7) illustrates Tank's Temperature (^{o}C) Distribution in contour plot get it from the thermal analysis.

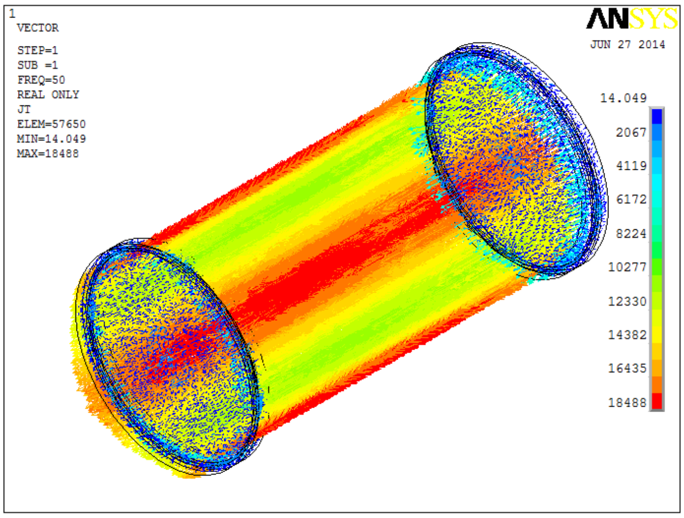

(a) Real component

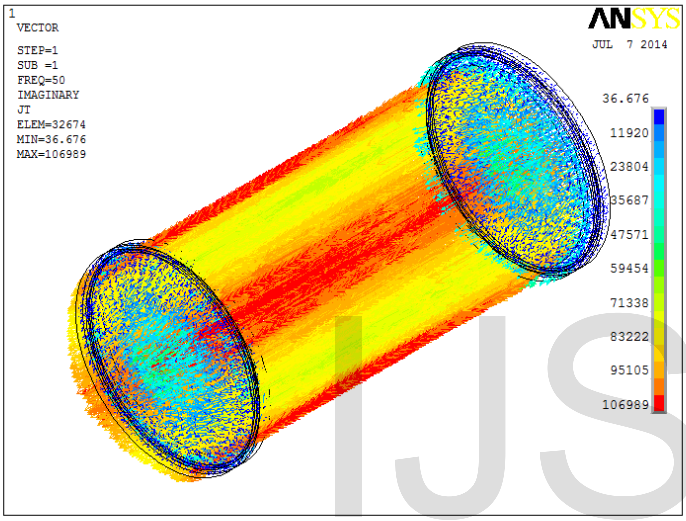

(b) imaginary component

Figure 5: Tank's with covers eddy currents density distribution vector plot from the harmonic analysis

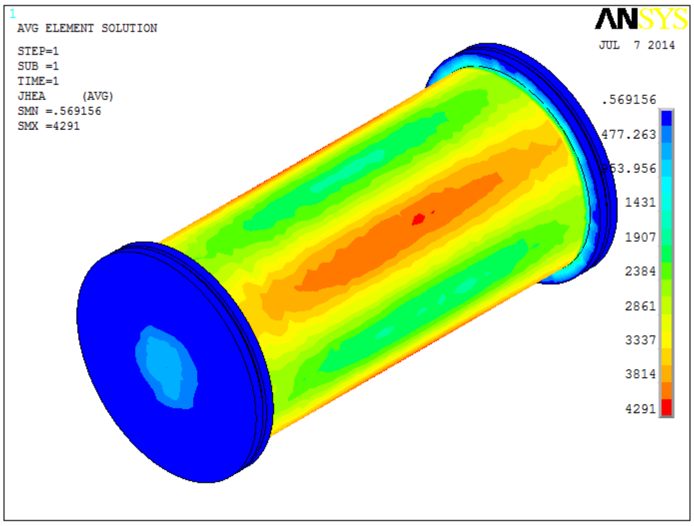

Figure 6: Tank's joule heat generation contour plot for the thermal analysis.

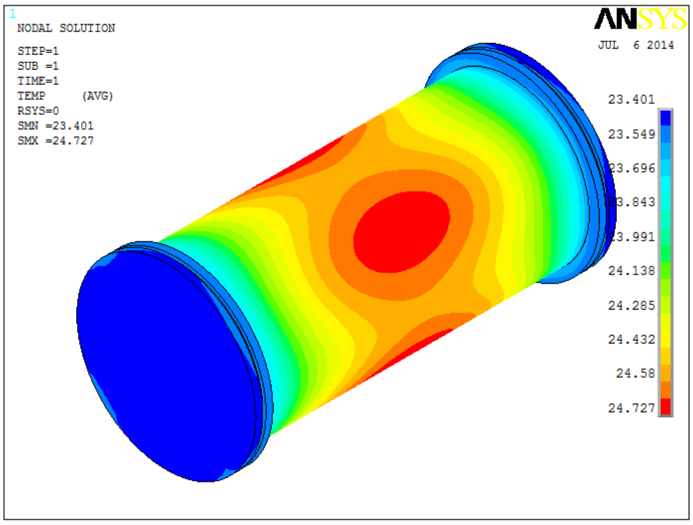

Figure 7: Tank's Temperature Distribution contour plot from thermal analysis.

Case (1): Fixed inner radius of GIB tank (rit) at (227mm) and Tank's thickness is changeable.

when we fixed the inner radius (r_{it}) of GIB tank (enclosure) at (227) mm, and tank's thickness is changeable to outside, we noticed that the tank's power losses increased with tank's thickness increased due to increased induced current in the GIB tank and then the increased heat generation lead to increase the tank's temperature as shown in table (3).

Tank thickness to outside mm	Tank r_{ot} mm	Tank $P_{loss,}$ Watts/m	Tank Avg.Temp ^oC
4	231	17.959	23.684
5	232	22.269	24.106
6	233	26.542	24.524
7	234	30.755	24.938
8	235	34.954	25.345

Table 3: At r_{it}=227mm and Tank's thickness is changeable

Case (2): Fixed outer radius of GIB tank (r_{ot}) at (233mm) and Tank's thickness is changeable.

In this case, when we fixed the outer radius (r_{ot}) of GIB tank (enclosure) on (233) mm, and tank's thickness is changeable to inside, we noticed that the tank's power losses increased with tank's thickness increased due to increased induced current in the GIB tank and then the increased heat generation lead to increase the tank's temperature, as shown in table (4).

Table 4: At r_{ot}=233mm and Tank's thickness is changeable

Tank Thickness to Inside mm	Tank r_{it} mm	Tank $P_{loss,}$ Watts/m	Tank Avg.Temp. ^oC
4	229	17.850	23.657
5	228	22.171	24.088
6	227	26.542	24.524
7	226	30.884	24.961
8	225	35.193	25.392

4.2 Case Study Two: T-Shape GIB Model

A. Side Current Feed to the GIB Main Conductor

Figures (8-10) are belonged to the (T-Shape GIB Model, side current feeding to the main Conductor), with the following dimension for GIB tank, inner radius=227mm & outer radius=233mm. Figure (8) illustrates the eddy currents distribution in the GIB tank (enclosure) get it from the harmonic analysis in contour plots for real and imaginary solution.

Figures (9 and 10) illustrate heat generation and temperature distribution for the GIB tank without covers in contour plot.

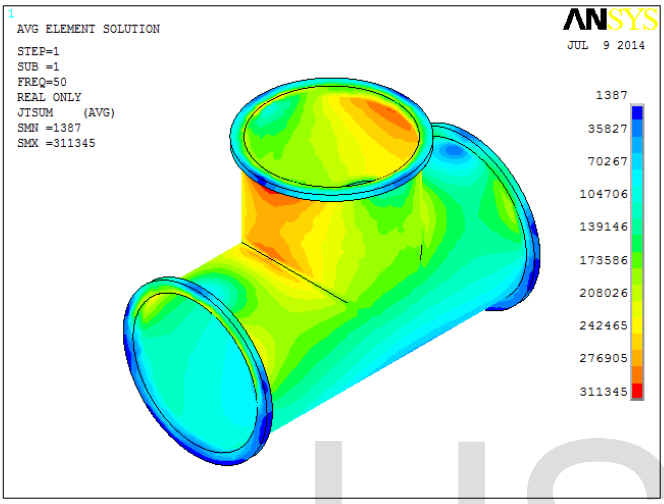

(a) Real component

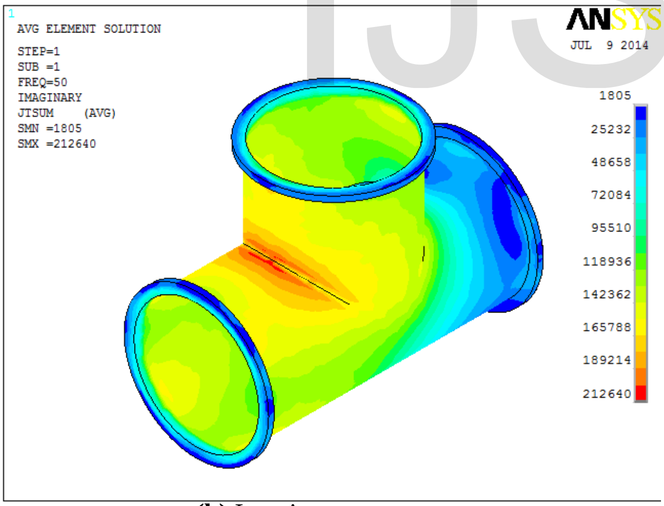

(b) Imaginary component

Figure 8: Tank's current density distribution contour plot for the harmonic analysis.

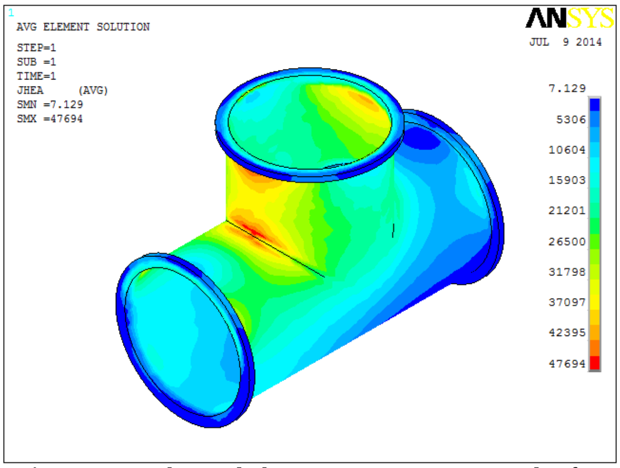

Figure 9: Tank's joule heat generation contour plot for thermal analysis.

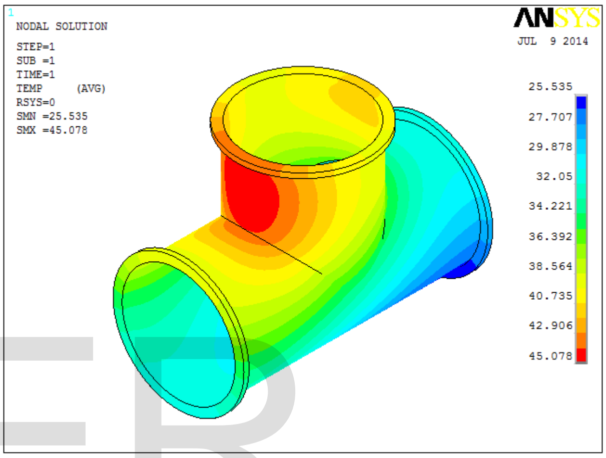

Figure 10: Tank's Temperature Distribution contour plot from the thermal analysis

B. Top Current Feed to the GIB Main Conductor

Figures (11-13) are belonged to the (T-Shape GIB Model, top current feeding to the main Conductor), with the following dimension for GIB tank, inner radius=227mm & outer radius=233mm.

Figure (11) illustrates the eddy currents distribution in the GIB tank (enclosure) get it from the harmonic analysis in contour plots for real and imaginary solution. Figures (12 and 13) illustrate heat generation and temperature distribution for the GIB tank without covers in contour plot get it from the thermal analysis.

In T-shape GIB, cases (A) and (B), we noticed that the tank's power losses depends on the way of GIB conductor feed (current direction flow), we notice the tank's power losses in the top feeding way (case B) is more than the tank's power losses in side feeding way (case A). Then the tank's power losses and then tank temperature distribution in T-shape GIB depends on the way of feeding and the value of current which feed. Table (5) shows comparison between side and top current feed at GIB Tank: inner radius is 227mm, tank thickness to inside be 6 mm and outer radius is 233mm.

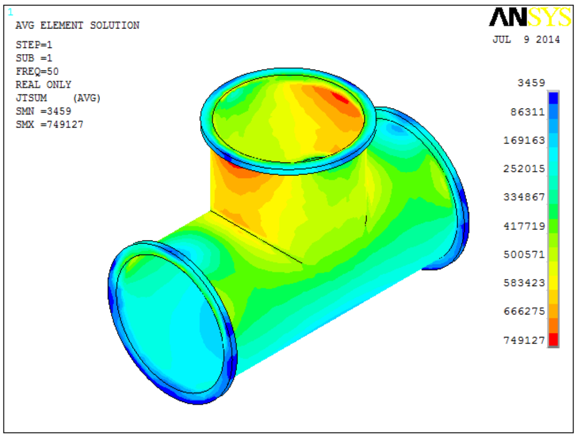

(a) Real component

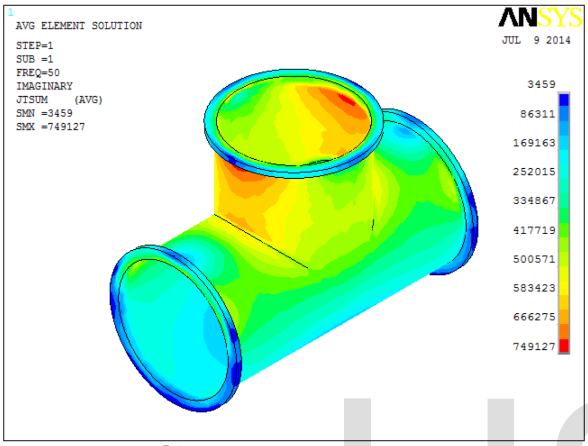

(b) Imaginary component

Figure 11: Tank's current density distribution contour plot for the harmonic analysis.

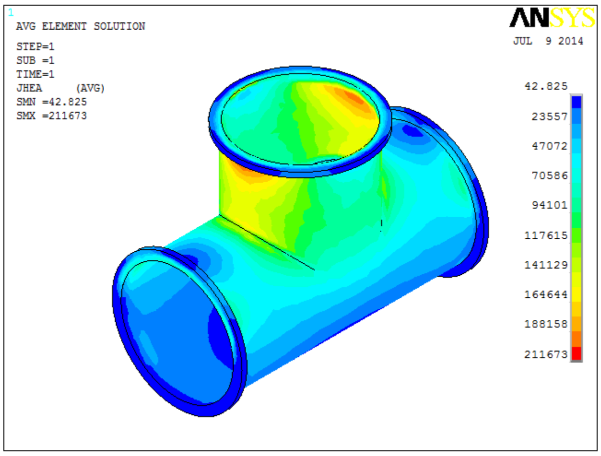

Figure12: Tank's joule heat generation contour plot for the thermal analysis.

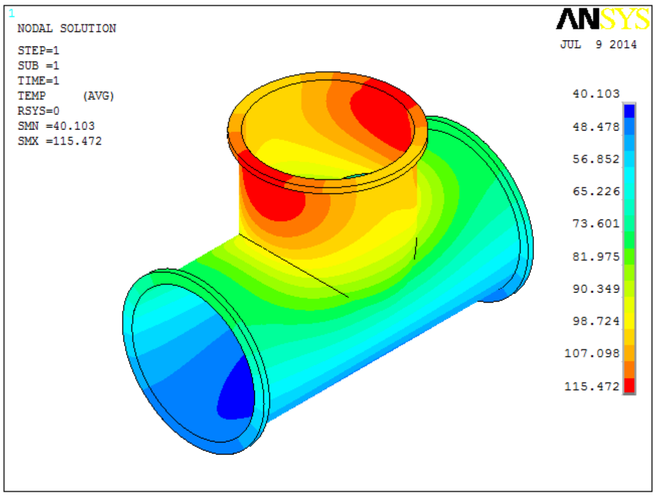

Figure 13: Tank's Temperature Distribution contour plot from the thermal analysis

Table5: Comparison between side and top current feed

GIB Tank (SS)			4000A rms, 50 Hz GIB Conductor (Al)	
Shape Model	Tank P_{loss}, Watts	Tank Avg. Temp. ^oC	Conductor P_{loss}, Watts	Conductor Avg. Temp. ^oC
Side feeding	163.821	33.580	123.975	42.860
Top feeding	666.977	68.650	135.398	45.468

5. Conclusion

The power of ANSYS package leads to use it to build the 3D model, the 3D finite element model and analysis the gas insulated busbar. The power losses are calculated by the magnetic fields analysis and are used as input data for the thermal analysis.

The temperature distribution is predicted by coupled magneto-thermal finite element analysis. Many tests and analysis are carried on this model and the results obtained are evaluated to get the optimum design. This work deals with the influence of GIB enclosure's geometry parameters like (thickness and shape) on the power losses and temperature distribution of gas insulated busbars of substations having separately enclosed busbars. From results, we see, the eddy current losses and the outer field can be reduced by optimizing the substation geometry. The proposed method in this paper can be used as a practical way to get the magneto-thermal analysis for the electromagnetic devices.

References

[1] M. Moallem and R. jafari," Transformation method in the coupled FE Magneto-thermal filed", IEEE Trans. Magnetics, Vol. 34, No. 5, pp.3126-3128, September. 1998.

[2] B. Novák, "Geometry optimization to reduce enclosure losses and outer magnetic field of gas insulated busbars", Elsevier, Electric Power Systems Research 81 (2011) 451–457.

[3] V. Garg and J. Weiss, "Magneto-Thermal Coupled Finite Element Calculation in Multiconductor Systems", IEEE *Trans.* MAG-23, No.5, pp.3296-3298, 1987.

[4] V. Hatziathanassiou and D. Labridis, "Coupled Magneto-Thermal Field Computation in Three-Phase Gas Insulated Cables", Arch. Electrotech, Vol.7 No.4, pp.285-292, May 1993.

[5] OSZKAR BIRO and KURT PREIS, "On the Use of the Magnetic Vector Potential in the finite element analysis of three-dimensional eddy currents" *IEEE Trans. Magnetic*, vol. 25, NO.4, July. 1989.

[6] S. L. Ho, Y. Li, and X. Lin, "Calculations of eddy current, fluid, and thermal fields in an air insulated bus duct system", *IEEE Trans. Magn.*, vol. 43, no. 4, pp. 1433–1436, Apr. 2007.

[7] S. L. Ho, Y. Li, and X. Lin, "A 3-D study of eddy current field and temperature rises in a compact bus duct system", *IEEE Trans. Magn.*, vol. 42, no. 4, pp. 987–990, Apr. 2006.

[8] J.H. Yoon, H.S. Ahn, J. Choi, I.S. Oh, "An estimation technology of temperature rise in GIS bus bar using three-dimensional coupled-field multi-physics", in: Proceedings of the IEEE ISEI, pp. 432–436, 2008.